AMERICAN SOCIETY FOR MICROBIOLOGY | mBio®

RESEARCH ARTICLE
Host-Microbe Biology

Dissecting Flavivirus Biology in Salivary Gland Cultures from Fed and Unfed *Ixodes scapularis* (Black-Legged Tick)

Jeffrey M. Grabowski,[a] Olof R. Nilsson,[b] Elizabeth R. Fischer,[c] Dan Long,[d] Danielle K. Offerdahl,[a] Yoonseong Park,[e] Dana P. Scott,[d] Marshall E. Bloom[a]

[a]Biology of Vector-Borne Viruses Section, Laboratory of Virology, Rocky Mountain Laboratories, NIAID/NIH, Hamilton, Montana, USA
[b]Salmonella-Host Cell Interactions Section, Laboratory of Bacteriology, Rocky Mountain Laboratories, NIAID/NIH, Hamilton, Montana, USA
[c]Microscopy Unit, Research and Technologies Branch, Rocky Mountain Laboratories, NIAID/NIH, Hamilton, Montana, USA
[d]Rocky Mountain Veterinary Branch, Rocky Mountain Laboratories, NIAID/NIH, Hamilton, Montana, USA
[e]Department of Entomology, Kansas State University, Manhattan, Kansas, USA

ABSTRACT The *Ixodes scapularis* tick transmits a number of pathogens, including tick-borne flaviviruses (TBFVs). In the United States, confirmed human infections with the Powassan virus (POWV) TBFV have a fatality rate of ~10% and are increasing in incidence. Tick salivary glands (SGs) serve as an organ barrier to TBFV transmission, and little is known regarding the location of TBFV infection in SGs from fed ticks. Previous studies showed *I. scapularis* vanin (*VNN*) involved with TBFV infection of *I. scapularis* ISE6 embryonic cells, suggesting a potential role for this gene. The overall goal of this study was to use SG cultures to compare data on TBFV biology in SGs from fully engorged, replete (fed) ticks and from unfed ticks. TBFV multiplication was higher in SGs from fed ticks than in those from unfed ticks. Virus-like particles were observed only in granular acini of SGs from unfed ticks. The location of TBFV infection of SGs from fed ticks was observed in cells lining lobular ducts and trachea but not observed in acini. Transcript knockdown of *VNN* decreased POWV multiplication in infected SG cultures from both fed and unfed ticks. This work was the first to identify localization of TBFV multiplication in SG cultures from a fed tick and a tick transcript important for POWV multiplication in the tick SG, an organ critical for TBFV transmission. This research exemplifies the use of SG cultures in deciphering TBFV biology in the tick and as a translational tool for screening and identifying potential tick genes as potential countermeasure targets.

IMPORTANCE Tick-borne flaviviruses (TBFVs) are responsible for more than 15,000 human disease cases each year, and Powassan virus lineage 2 (POWV-L2) deer tick virus has been a reemerging threat in North America over the past 20 years. Rapid transmission of TBFVs in particular emphasizes the importance of preventing tick bites, the difficulty in developing countermeasures to prevent transmission, and the importance of understanding TBFV infection in tick salivary glands (SGs). Tick blood feeding is responsible for phenomenal physiological changes and is associated with changes in TBFV multiplication within the tick and in SGs. Using SG cultures from *Ixodes scapularis* female ticks, the primary aims of this study were to identify cellular localization of virus-like particles in acini of infected SGs from fed and unfed ticks, localization of TBFV infection in infected SGs from fed ticks, and a tick transcript (with associated metabolic function) involved in POWV-L2 infection in SG cultures.

KEYWORDS Powassan, RNA interference, application, blood feeding, control, countermeasure, flavivirus, metabolism, saliva, salivary gland, tick, tick-borne pathogens

Citation Grabowski JM, Nilsson OR, Fischer ER, Long D, Offerdahl DK, Park Y, Scott DP, Bloom ME. 2019. Dissecting flavivirus biology in salivary gland cultures from fed and unfed *Ixodes scapularis* (black-legged tick). mBio 10:e02628-18. https://doi.org/10.1128/mBio.02628-18.

Editor Thomas E. Morrison, University of Colorado School of Medicine

Address correspondence to Jeffrey M. Grabowski, jgrabows25@gmail.com.

This article is a direct contribution from a Fellow of the American Academy of Microbiology. Solicited external reviewers: Alan Barrett, University of Texas Medical Branch; Aaron Brault, Centers for Disease Control and Prevention.

Received 28 November 2018
Accepted 12 December 2018
Published 29 January 2019

Vector-borne illnesses have increased since 2004 in the United States, and cases of tick-borne disease have more than doubled in the last 13 years (1). Powassan virus (POWV) is the only endemic tick-borne flavivirus (TBFV) in North America, and cases of POWV infection have been on the increase in the United States since 1999 (2–6). The cases have been identified in the upper Midwest and upper East Coast states of the United States. POWV infections can be asymptomatic or symptomatic. The latter may be associated with severe neurological disease, including meningoencephalitis, and with a case fatality rate of approximately 10%. Additionally, long-term neurological sequelae may arise (7, 8).

There are currently two genetic lineages of POWV: lineage 1 (POWV-L1) and lineage 2 (deer tick virus; POWV-L2). The lineages are suggested to have different ecological life cycles, including different tick vectors, mammalian hosts, and habitats (6, 8). POWV-L1 has been isolated from *Haemaphysalis longicornis*, *Ixodes spinipalpis*, *Ixodes marxi*, and *Ixodes cookei* (8–14). POWV-L2 has been isolated from the black-legged tick, *Ixodes scapularis* (15–21) and the Rocky Mountain wood tick, *Dermacentor andersoni* (20, 22). Similarly to other tick-borne viruses (TBVs), POWV can be transmitted to a mammal host from an infected tick in as little as 15 min (15, 23). Other TBFVs have been identified in tick saliva and in the cement cone created during attachment and feeding (24, 25). These observations suggest that infectious virus is present in salivary glands (SGs) prior to feeding and can thus be transmitted in the early stage of feeding. Thus, salivary gland-TBFV (SG-TBFV) interactions, SG saliva production, and TBFV secretion are of key importance in understanding mechanisms of TBFV transmission.

The SG of the female ixodid tick is made up of a series of ramifying lobular ducts with three types of acini. Tracheal ducts branch into tracheoles that infiltrate tissues, including those of SGs, and are involved in respiration (26). The type 1 acini are agranular and nonsecretory in nature; they are implicated in osmoregulation and ion uptake. The type 2 and 3 acini are granular and secretory in nature; they are involved in production and secretion of saliva (27–29). The type 2 acinus is composed of cell types a, b, and c, whereas the type 3 acinus has cell types d, e, and f (30, 31). Type a cells have been implicated in release of secretory granules (29) and of molecules associated with the cement cone (30, 32) in response to blood feeding. Type b cells have been linked with secretory activity (29) and secretion of glycoproteins (30, 32). Type d cells have been associated with release of secretory granules (29). Both type d and type e cells are thought to contribute to the formation of the cement cone (30, 33).

There are three stages in blood feeding; the feeding lesion is formed during the preliminary phase (24 to 36 h), the slow-feeding phase occurs between days 5 and 10, and the final rapid feeding phase occurs between h 12 and h 24 (34–36). During feeding, the SGs undergo marked changes. These include increased protein synthesis as well as induction of apoptotic and autophagic responses (30, 37). In addition, the size of the type 2 and 3 acini increases in comparison to that of type 1 acini during tick blood feeding (29). Because the transmission of TBFVs occurs in the first feeding phase, identification of the specific cell types that are targets for TBFV infection, especially within acini types 2 and 3, may pinpoint how TBFVs are shed into saliva.

Ticks infected during blood feeding develop higher levels of virus both in the whole ticks and in SGs (25, 38–40). Booth et al. identified Thogoto virus (THOV; a member of the *Orthomyxoviridae* family) antigen in the lumen of granular acini (type 2/3) and basement membranes of all three acini types (40). This suggests that all three acini types may be susceptible to TBV infection. Grabowski et al. observed antigens of Langat virus (LGTV), a model TBFV, and POWV-L1 in granular acini and in lobular ducts of infected SG cultures from unfed *I. scapularis* female ticks (41). However, the precise cellular localization of viral antigen and virions was not determined. Furthermore, the cell types that are susceptible to TBFV infection in SGs from fed *I. scapularis* female ticks remain unknown.

Given the crucial role of SG biology in TBFV transmission, another important issue is defining changes in the tick transcriptome and proteome following TBFV infection of SGs. Identifying key changes in cellular pathways may suggest targets for possible

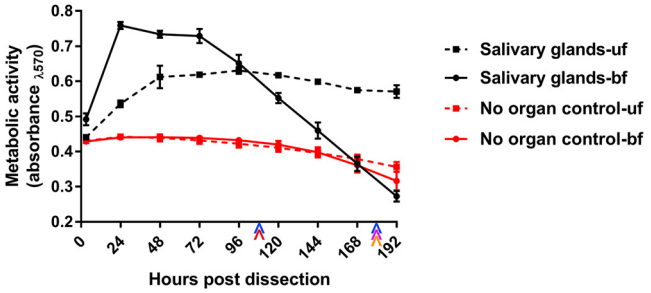

FIG 1 Metabolic viability of SGs from fed (bf) and unfed (uf) ticks in culture. Resazurin salt-based viability readings (41, 44, 65) were completed with one SG pair with its corresponding control for all time points. Error bars represent standard errors of the means (SEM), and data are representative of results from 1 to 3 machine replicates (replicate reads from the plate reader) for each sample during viability reads of 2 to 4 biological replicates. Colored arrowheads denote time points used in SG culture-based analyses completed in this study as follows: blue, infectious virus multiplication; magenta, confocal imaging of $LGTV^{GFP}$ expression; orange, transmission electron microscopy imaging; red, dsRNA-mediated RNA interference analysis.

countermeasures. Although data on SG transcripts associated with LGTV infection of whole nymphal *I. scapularis* ticks have been published previously (42, 43), it is not known if the same transcripts are implicated in adult SGs. Additionally, another study functionally associated a small subset of transcripts in *I. scapularis* ISE6 cells with LGTV infection (44). Specifically, transcript knockdown of predicted *I. scapularis* carbon-nitrogen hydrolase/pantetheine hydrolase/vanin-like, or vanin (*VNN*), reduced LGTV genome replication and infectious multiplication. It is important to know if transcript knockdown of *VNN* would reduce POWV infection in tick SG organ cultures.

The overall goals of this study were to compare TBFV biology in SGs from fed ticks to that in SGs from unfed ticks and to further evaluate the useful application of SG cultures in defining possible targets for countermeasure development. Utilizing SG cultures, the aims of this study were as follows: (i) to compare results corresponding to SG viability, TBFV multiplication, and size of granular acini from fed versus unfed female *I. scapularis* ticks; (ii) to utilize green fluorescent protein (GFP)-tagged LGTV ($LGTV^{GFP}$) to identify locations of TBFV multiplication in SGs from fed ticks; (iii) to identify cellular localization of virus-like particles (VLPs), or virions, in cell types of TBFV-infected SG acini from fed and unfed ticks; and (iv) to observe effects of *VNN* transcript knockdown on multiplication of pathogenic POWV in SG cultures from fed and unfed ticks.

RESULTS

Viability and TBFV multiplication in SG cultures from fed and unfed ticks. The studies undertaken required a careful determination of the viability of short-term SG cultures from both fully engorged, replete (fed) *I. scapularis* ticks and unfed *I. scapularis* ticks (41, 45). Thus, we compared the levels of metabolic activity of cultures from fed and unfed ticks. SGs from fed ticks exhibited greater metabolic activity 24 to 72 h postculture (hpc) than SGs from unfed ticks. This may have been due in part to the size difference between SGs from fed ticks and SGs from unfed ticks. SG cultures from unfed ticks are metabolically viable longer (for up to 264 hpc [41]) than SGs from fed ticks (168 to 192 hpc) (Fig. 1). Thus, we decided to use 180 h as the final time point in this study.

We next compared levels of multiplication of the following three TBFVs in the culture model: LGTV, POWV-L1, and POWV-L2. All three replicated in SG cultures from fed and unfed ticks. Multiplication of all three was greater in cultures from fed ticks than in cultures from unfed ticks (Fig. 2). Interestingly, POWV-L2 replicated to higher levels than POWV-L1. Thus, each of the examined TBFVs was able to replicate in SG cultures from both fed and unfed ticks.

Morphology of acini from mock-infected and infected SG cultures from fed and unfed ticks. To compare the structures of acini from SG cultures from fed and unfed ticks, we utilized high-resolution light microscopy. Examination of semithin sections

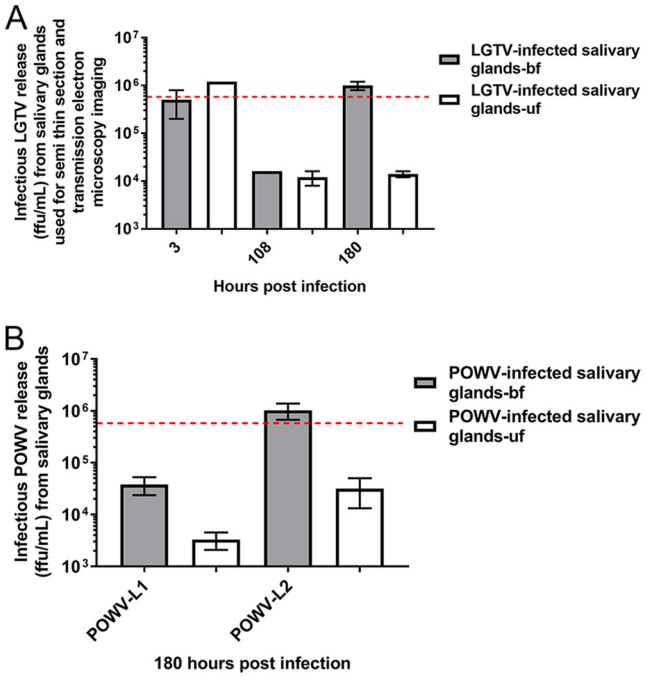

FIG 2 Infectious TBFV multiplication in SG cultures from fed (bf) and unfed (uf) ticks. (A) Quantitation of infectious virus multiplication with immunofocus assays was performed on supernatants collected from wells with one LGTV-infected SG pair from fed (gray box) and unfed (white box) ticks at 3, 108, and 180 h postinfection (hpi). The red dotted line denotes the initial inoculum of 5×10^5 focus-forming units (FFU) used for infections. Error bars represent means and ranges, and data are representative of results from two technical replicates of each sample for the immunofocus assays. (B) Subsequently, detection of infectious virus production with immunofocus assays was completed with supernatants collected from wells with POWV-L1- or POWV-L2-infected SG pairs from fed (gray box) and unfed (white box) ticks at 180 hpi. The red dotted line denotes the level measured in a control well without SGs (initial inoculum) that was collected at 3 hpi. "POWV-L1" denotes Powassan virus lineage I (LB strain), and "POWV-L2" denotes Powassan (deer tick) virus lineage II (Spooner strain). Error bars represent standard errors of the means, and data are representative of results from 2 technical replicates for each sample for the immunofocus assays performed with 2 to 3 biological replicates.

(Fig. 3) confirmed that the SG cultures maintained the basic morphology found *in vivo* ixodid ticks (29, 46). The SG cultures from the unfed ticks provided similar structures with respect to the specific cell types and features found within granular acini of ixodid female ticks (29, 46). Depending on how the sections were cut, lumen of acini and lobular ducts were observed. In addition, the semithin sections also confirmed that SG cultures of the fed ticks had and maintained larger degranulated, granular acini (associated with the blood feeding process and apoptotic events [29]) than the granular acini of the unfed tick. Degranulated acini (type 2 and/or 3) were obvious in mock- and LGTV-infected SG cultures from fed ticks (Fig. 3); the diameters were much larger than those seen with the granulated acini of SGs from unfed ticks (Fig. 3 and 4). There was no obvious difference between the mock- and LGTV-infected acini from fed and unfed ticks. This analysis confirmed that the structures of granular acini from SG cultures from fed and unfed ticks were similar to those of SGs from fed and unfed whole ticks and that infection did not obviously affect acini structure.

Localization of LGTV infection in SG cultures from fed and unfed ticks. TBFV replicated in SG cultures from both fed and unfed female *I. scapularis* ticks (Fig. 2). However, the location of TBFV infection in SGs of fed ticks is unknown. To determine this, we infected cultures from both fed and unfed ticks with LGTV^{GFP} and compared the cultures for determination of the location of the GFP signal by confocal imaging (Fig. 5; see also Movie S1 to S6). We considered the site of the GFP signal to represent the location of virus multiplication. As reported previously (41), autofluorescence was noted in the main lobular duct in SGs from both fed and unfed ticks (Fig. 5B and D; see

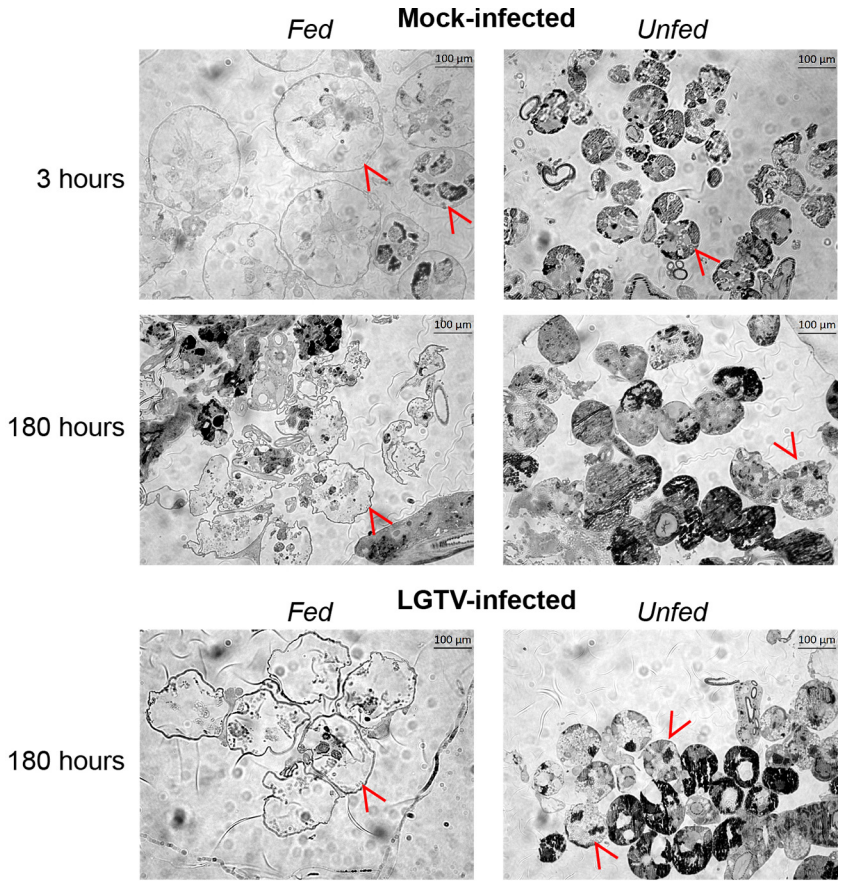

FIG 3 Granular acini of mock-infected and TBFV-infected SG cultures. Images are representative of semithin (1-μm-thick) sections taken at ×40 magnification of mock-infected and LGTV-infected SGs from fed/unfed ticks at 3 and 180 h postinfection (hpi). Also included are representative images of semithin (1-μm-thick) sections taken at ×40 magnification of LGTV-infected SGs from fed/unfed ticks at 180 hpi. Red arrowheads denote example granular acini in images. Scale bars in the upper right of each image represent 100 μm.

also Movie S2 and S4) and in small puncta within degranulated acini of fed ticks (Fig. 5B; see also Movie S2). No GFP signal was observed within degranulated acini in SGs from fed ticks (Fig. 5A; see also Movie S1). However, GFP expression was consistently seen in cells lining multiple tracheal and lobular ducts (Fig. 5A; see also Movie S1 and S5) throughout the SG. The tracheal ducts, involved in respiration, are not part of the SG apparatus but are often found intertwined with SGs (27, 47). The GFP expression around these ducts was often noted in areas where acini were attached. Taken together, these GFP results confirmed that SG cultures from fed ticks can support LGTV multiplication.

GFP expression of LGTV^{GFP} also was observed in granular acini and cells lining the lobular duct of SGs from unfed ticks (Fig. 5C and F; see also Movie S3 and S6). However, GFP expression in the cells lining the lobular ducts was not as extensive as that seen in fed ticks. Specifically, GFP expression was detected in type 2 acini and in apical epithelial cells of type 3 acini (Fig. 5F). LGTV^{GFP} was not apparent in acini of SGs of fed ticks but was evident in acini of SGs from unfed ticks. This further suggested that the acini harboring LGTV^{GFP} infection were granular (type 2 and/or 3) in nature since these types of acini are degranulated in fully engorged, replete ixodid ticks.

Finally, we examined thin sections prepared from SG cultures by transmission electron microscopy (TEM) imaging to identify VLPs. No structures resembling VLPs in size or appearance were observed in mock-infected SG cultures from fed or unfed ticks. VLPs consistent with flavivirus particles were identified in LGTV-infected SGs from unfed

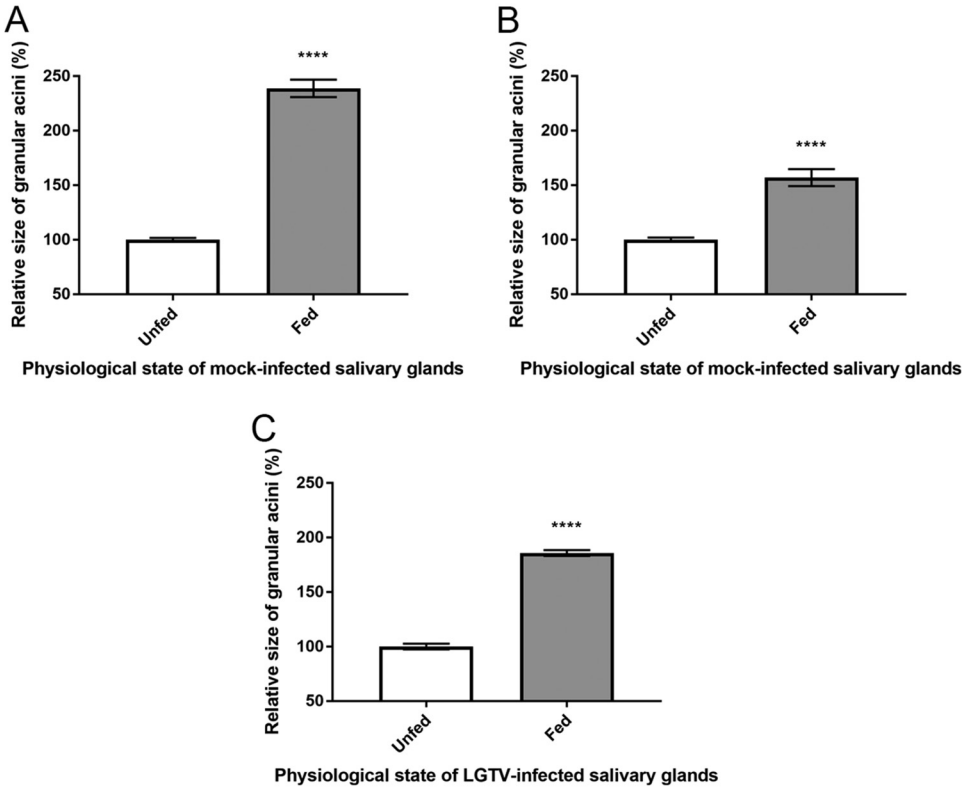

FIG 4 Relative size differences of granular acini from mock-infected and TBFV-infected SG cultures. (A and B) Diameters of granular acini of (A) mock-infected SGs from fed/unfed ticks at (A) 3 h postinfection (hpi) and (B) 180 hpi. (C) Diameters of granular acini of LGTV-infected SGs from fed/unfed ticks at 180 hpi derived from images of semithin (1-μm-thick) sections taken at $\times$40 magnification (Fig. 3). Results show size (longest measurable diameter) of granular acini of SGs from fed ticks relative to that of granular acini of SGs from unfed ticks. Error bars represent standard errors of means. Statistical analysis was performed using an unpaired *t* test, and data are representative of results from 8 to 68 measured granular acini (A to C). ****, $P \leq 0.0001$.

ticks; they were mostly within single-membrane bound vacuoles (Fig. 6; see also Fig. S1 in the supplemental material) but were also noted in a double-membraned vacuole (Fig. 6A and B) as well as in the lumen of granulated acini (Fig. 6G and H; see also Fig. S1). Since no VLPs were observed in mock-infected SG cultures, we concluded that they represented virions in LGTV-infected SGs. The extensive degranulation of granular acini of SGs from fed ticks precluded clear identification of virions from these cultures (Fig. S2). Nevertheless, our TEM analysis provided evidence of virion localization in granular acini of LGTV-infected SGs from unfed *I. scapularis* ticks.

The role of vanin in POWV-L2 multiplication in SG cultures. To identify whether *I. scapularis* vanin (*VNN*) transcript was involved in POWV-L2 infection of SGs in different physiological states, the effect on infectious POWV-L2 multiplication following *VNN* transcript knockdown was assessed. First, *VNN* transcript expression in SGs from fed and unfed tick was identified via two-step reverse transcription-PCR (RT-PCR) with pooled SGs. We observed amplification of *VNN* transcript in SGs from both fed and unfed ticks (Fig. S3) as previously observed in *I. scapularis* ISE6 cells (44). Next, double-stranded RNA (dsRNA) corresponding to *VNN* was created and transfected in POWV-L2-infected SG cultures to determine the effect on infectious virus multiplication. Transfection of 10 ng of *VNN* dsRNA in SG cultures from both fed and unfed ticks at 108 h postinfection (hpi) yielded relative reductions of *VNN* transcript levels by 70% and 50%, respectively (Fig. 7A and B). Additionally, these transfection conditions did not decrease the metabolic viability of the SGs in culture, but viability did increase in SG cultures from fed ticks (Fig. 7C and D). In completing these *VNN* dsRNA transfections in POWV-L2-infected SG cultures, a ($10^{0.5}$-fold to $10^{1.5}$-fold) reduction in infectious POWV-L2 mul-

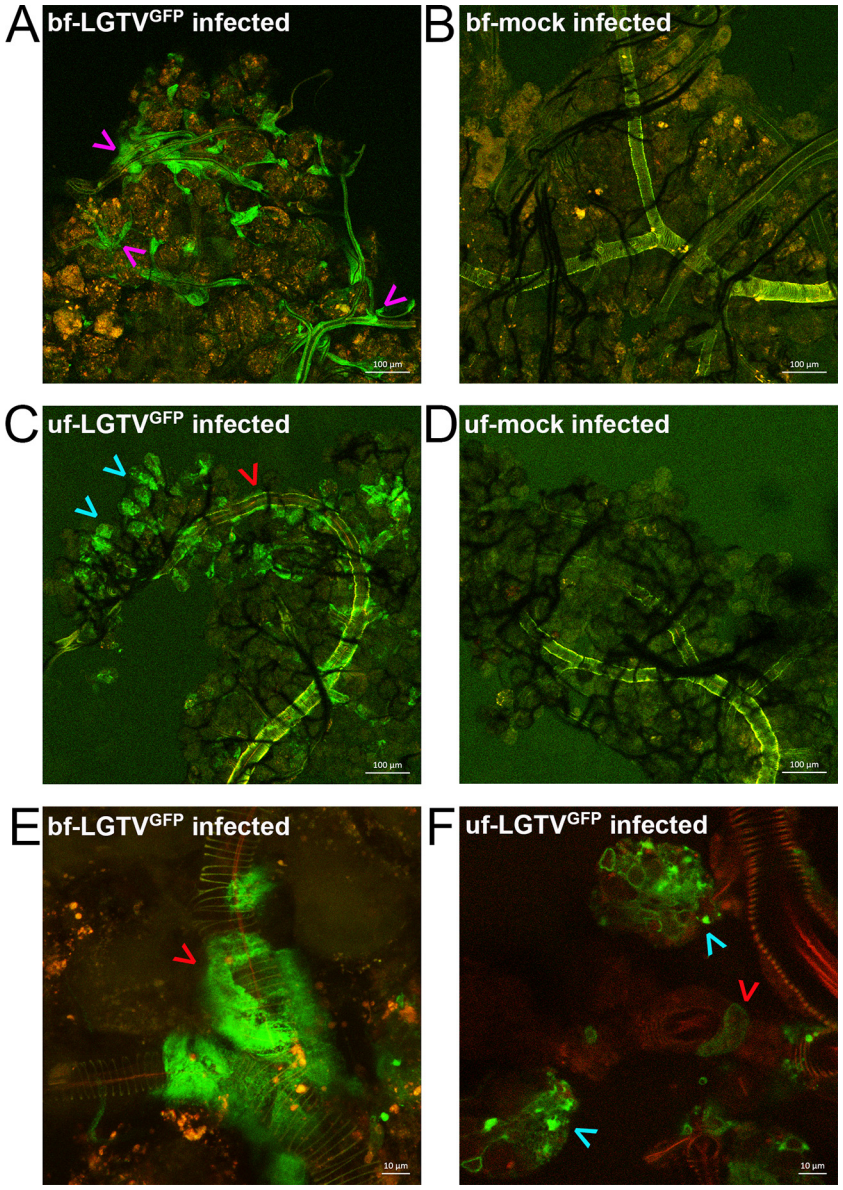

FIG 5 LGTV^{GFP} multiplication in infected SG culture from a fed tick (bf) and an unfed tick (uf). Magnification, ×10 (A, B, C, and D) or ×63 (E and F). A red filter was used to show the structure of the SGs. LGTV-expressed GFP (LGTV^{GFP}) is shown in green within the organ. Mock-infected organs were used for comparison, and autofluorescence was observed mostly within lobular duct. Magenta arrowheads denote GFP expression associated with cells surrounding tracheal ducts of SGs. Red arrowheads denote GFP expression associated with cells surrounding lobular ducts of SGs. Cyan arrowheads denote GFP expression within granular acini of SGs. (A and B) LGTV^{GFP}-infected SGs (A) and mock-infected SGs (B) from fed ticks at 180 hpi. (C and D) LGTV^{GFP}-infected SGs (C) and mock-infected SGs (D) from unfed ticks at 180 hpi. (E) Cells with GFP expression surrounding lobular duct of LGTV^{GFP}-infected SGs from fed tick are highlighted. (F) Cells with GFP expression inside granular acini and cells surrounding lobular duct of LGTV^{GFP}-infected SGs from unfed tick are highlighted. The scale bar in the lower right of each image represents either 100 μm (A, B, C, and D) or 10 μm (E and F).

tiplication was observed in SGs from both fed and unfed ticks, respectively (Fig. 8A and B; see also Fig. S4). These transcript knockdown experiments suggested that *VNN* may indeed be implicated in pathogenic TBFV infection of SG tissue.

DISCUSSION

We previously reported that salivary glands dissected from unfed adult female *I. scapularis* ticks could be successfully cultured and supported multiplication of TBFVs

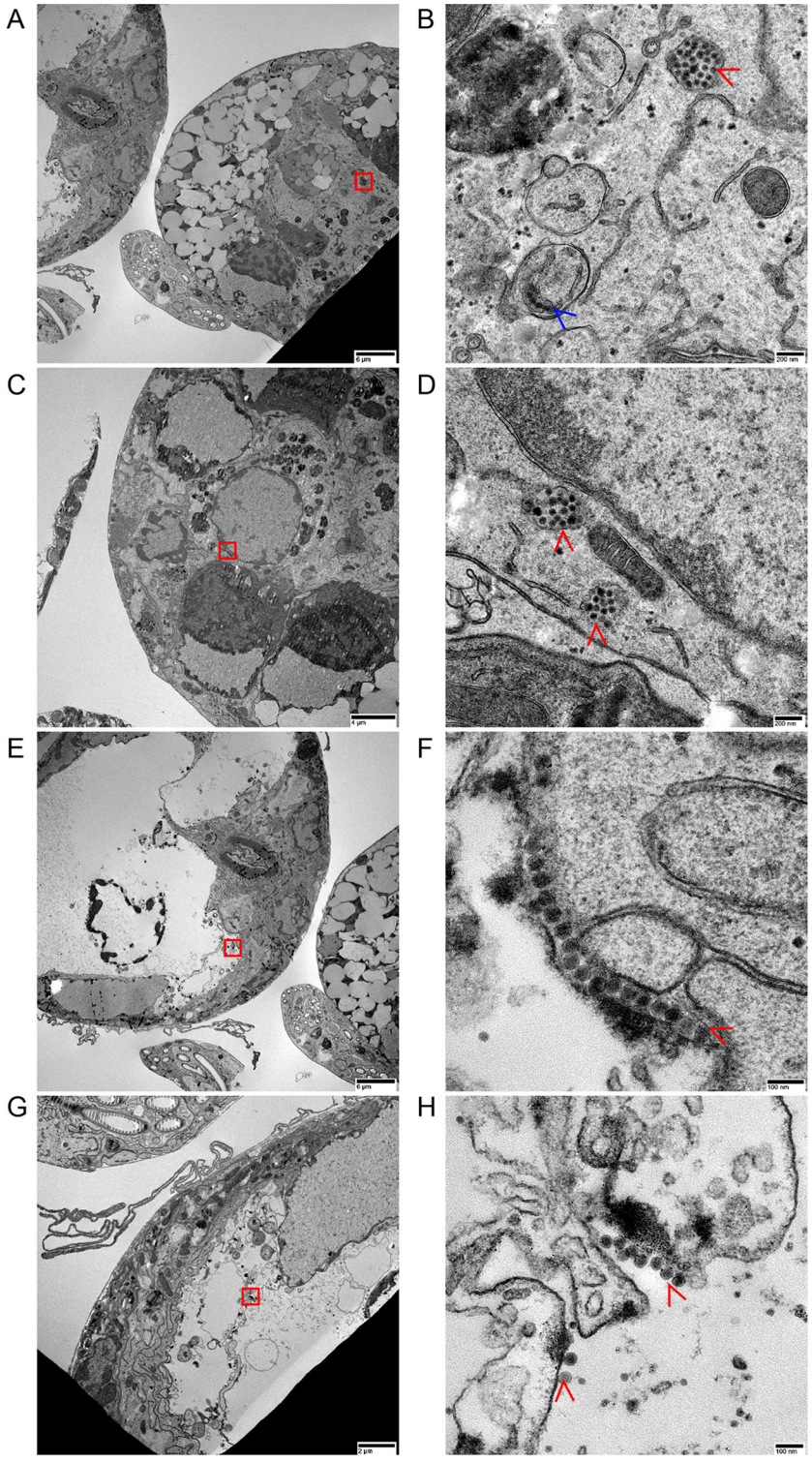

FIG 6 Observation of virus-like particles (virions) in LGTV-infected SG cultures from unfed ticks. (A to F) Transmission electron microscopy images of a granular acinus with a highlighted area (red box) (A, C, and E), showing a double-membraned vacuole (blue arrow) (B) and vacuoles (red arrowheads) with virions inside (B, D, and F). (G and H) In the lumen of a granular acinus (G), virions were identified outside vacuoles (red arrowheads) (H). The acini in panels A and C are suggested to be type 3 acini cut at the basal and apical epithelial cell regions, respectively. The acinus in panel E is suggested to be a type 2 acinus cut at the basal region. Images were taken at ×700 and ×15,000 magnification, and scale bars represent 6 μm and 200 nm for panels A and B, respectively. Images represent ×1,200, ×15,000, ×700, and ×40,000 magnification for panels C, D, E, and F, respectively, and scale bars represent 4 μm, 200 nm, 6 μm, and 100 nm for panels C, D, E, and F, respectively. Images represent ×2,000 and ×30,000 magnification for panels G and H, respectively,

(Continued on next page)

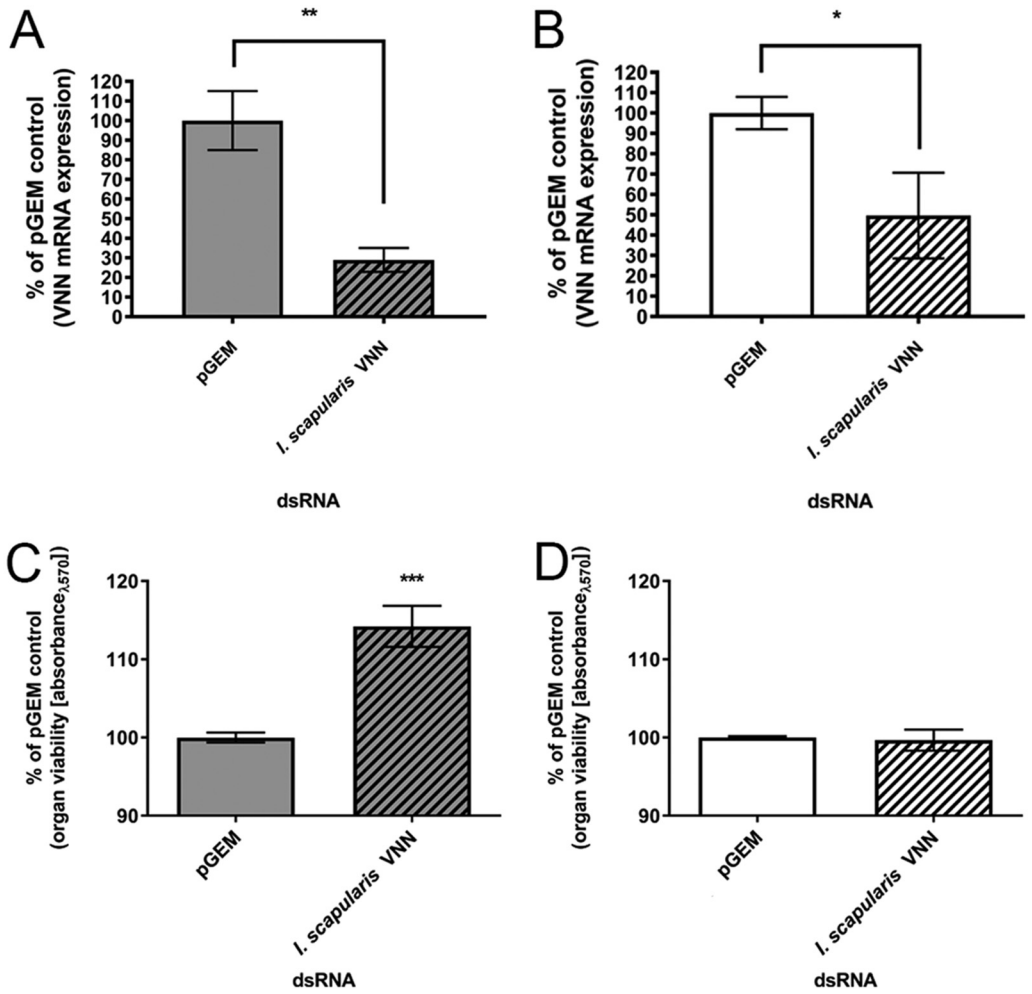

FIG 7 Transfection of dsRNA corresponding to *VNN* transcript and effect on transcript knockdown and viability of SG cultures. (A and B) Transfection of a SG pair from fed ticks (A) or unfed ticks (B) with 10 ng dsRNA for 108 h was completed. To determine transcript knockdown, three SG pairs and six SG pairs from fed and unfed ticks, respectively, were transfected independently and pooled. Total RNA was extracted followed by cDNA amplification via two-step RT-PCR. mRNA levels were normalized to *I. scapularis β-actin* and are expressed relative to the percentage of negative pGEM control cDNA. Results show relative expression levels of the *VNN I. scapularis* gene following knockdown (striped bars) relative to the pGEM dsRNA negative control (solid bars). Results represent 2 to 3 machine replicates (replicate reads from the real-time thermocycler) of RT-qPCR derived from the pooled, transfected SG pairs from fed and unfed ticks described above. Error bars represent means with range values. Statistical analysis was performed using an unpaired *t* test for comparisons between the negative pGEM control and dsRNA treatment for *VNN*. (C and D) To determine the associated transcript knockdown effect on organ viability, transfections were completed independently as described above with SG pairs from (C) fed ticks and (D) unfed ticks. Results show levels of organ viability following associated transcript knockdown of *I. scapularis VNN* (striped bars) relative to those seen with the negative pGEM control (solid bars). Results represent 3 to 4 machine replicates (replicate reads from the plate reader) of 2 to 3 biological replicates. *, $P \leq 0.05$; **, $P \leq 0.01$; ***, $P \leq 0.001$. Error bars represent standard errors of the means (SEM). Statistical analysis was performed using an unpaired *t* test for comparisons between the negative pGEM control and dsRNA treatment for *VNN*. Abbreviations: *VNN*, carbon-nitrogen hydrolase/vanin-like; pGEM, pGEM plasmid (negative control).

(41). In the current study, we extended that work to specifically localize sites of virus multiplication. Furthermore, we compared levels of virus infection in SG cultures from fed and unfed adult female ticks, representing two vastly different physiological states. In addition, we showed that a gene (*VNN*) implicated in TBFV multiplication in tick cell culture reduced viral production in SG cultures.

FIG 6 Legend (Continued)
and scale bars represent 2 μm and 100 nm for panels G and H, respectively. These virions were not observed in mock-infected SG cultures from unfed ticks. In addition, no virions were clearly identified in the degranulated acini of LGTV-infected SG cultures from fed ticks (Fig. S2).

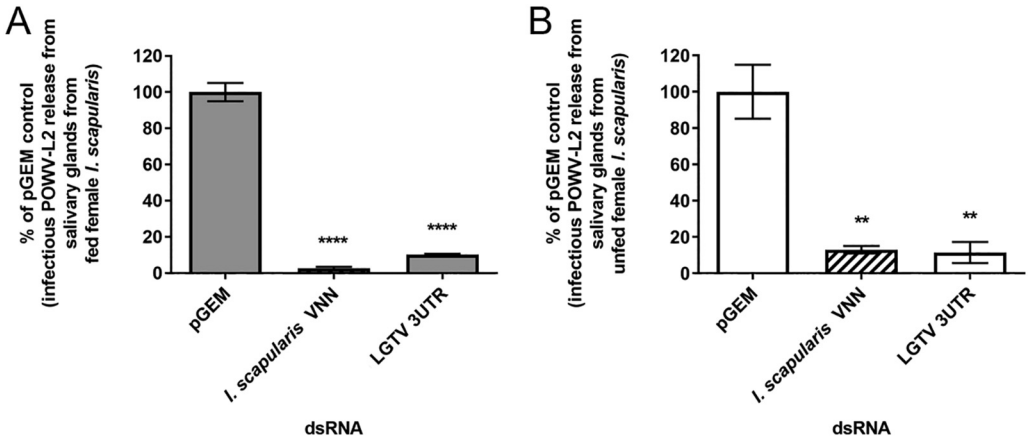

FIG 8 Transfection of dsRNA corresponding to *VNN* transcript and effect on infectious POWV-L2 multiplication from infected SG cultures. pGEM, pGEM plasmid (negative control); LGTV 3UTR, 3′ UTR of LGTV strain TP21 (positive control). Transfection of POWV-L2-infected SG pair from (A) fed tick and (B) unfed tick with 10 ng pGEM dsRNA, LGTV 3′ UTR dsRNA, and *VNN* dsRNA (striped bars). Transfections of SGs were completed for 108 h before supernatants were collected for immunofocus assays, which were normalized to the pGEM dsRNA negative-control response. An unpaired *t* test was completed to compare FFU per milliliter of the *VNN* dsRNA and LGTV 3′ UTR dsRNA to that for the pGEM dsRNA negative control. Error bars represent standard errors of the means, and data are representative of results from 2 technical replicates for each sample for the immunofocus assays of 2 biological replicates. **, $P \leq 0.01$; ****, $P \leq 0.0001$. Abbreviations: *VNN*, carbon-nitrogen hydrolase/vanin-like; pGEM, pGEM plasmid (negative control); LGTV 3UTR, 3′ UTR of LGTV (positive control).

LGTV and both lineages of POWV replicated well in cultures from both fed and unfed ticks. Virus production was greater in the cultures from fed ticks (Fig. 2), a finding that mirrored results from infected whole ticks (25, 38–40). POWV-L2 (deer tick virus) replicated to higher levels than POWV-L1 (Fig. 2B). This may be suggestive of the possibility that the two lineages of POWV may multiply differently in *I. scapularis* and that the results may reflect differences in transmission efficiency. This is an interesting observation since *I. scapularis* is considered a natural vector for POWV-L2 (8, 16–21), whereas other ixodid tick species (*H. longicornis*, *I. spinipalpis*, *I. cookei*, and *I. marxi*) are implicated in maintenance of POWV-L1 (8–14). POWV-L2 has been found in natural populations of *D. andersoni* (20, 22), but the natural transmission cycle of POWV with this tick species remains unclear. Further studies are required in order to compare the levels of growth of TBFV (LGTV and both POWV lineages, including multiple isolates/strains of each) in SG cultures from multiple tick species and in whole ticks of different species to determine if there are definable biological differences. This would help address potential transmission barriers of POWV in the multiple tick species (of the genera *Ixodes*, *Dermacentor*, *Amblyomma*, and *Haemaphysalis*) that are found in North America.

We used several methods to localize virus multiplication and virus in SG cultures. In the cultures from unfed ticks, viral gene expression was localized to cells lining lobular ducts and cells found in granular acini type 2 or 3 (Fig. 5C and F; see also Movie S3 and S6 in the supplemental material). These cells are involved with secretory activity in SGs, and virus in these cells would be available for rapid release into the saliva. This observation may be relevant since virus can be transmitted as soon as 15 min after initiation of feeding (15, 23). As noted in Results, both types of granular acini contain several different types of secretory cells, and it would be informative to determine if specific cell types support virus multiplication. This determination might better define specific targets for countermeasures against TBFV infections. VLPs consistent with LGTV virions were observed in the cells and lumen of granular acini, supporting the idea of a role of these structures in virus multiplication. The cells containing the virions did not exhibit the extreme membrane expansion characteristic of LGTV multiplication in mammalian cells, a finding that was also noted previously in a report of LGTV infection of *I. scapularis* embryonic cells (48).

SG cultures from fed ticks represent a metabolic state that is very different from that seen with unfed ticks. Blood feeding is associated with an increase in SG protein synthesis as well as with the presence of virions when the SGs have secreted their salivary components. Also, apoptosis and autophagy are initiated in SGs as a replete, fed tick prepares to molt or lay eggs. Our observations in the SG cultures reflected this marked change as evidenced by the extensive degranulation of the acinus and by the increase in the size of the granular acinus (Fig. 3 and 4; see also Fig. S2 in the supplemental material). Furthermore, we did not observe virions or obvious viral gene expression in degranulated acinar cells as manifested by signal from LGTV^{GFP}. However, GFP signal was apparent in cells of the lobular ducts and tracheal ducts from the fed tick cultures (Fig. 5A and E; see also Movie S1 and S5). Perhaps these are sites in which virus is maintained in the tick as it progresses through molting or laying eggs. the presence of LGTV^{GFP} in the tracheal cells may also imply that this virus can use the tracheal network connecting different organs as a route for infection, as in the case of baculovirus infection in caterpillar (49). In future studies, we plan to prepare TBFV-infected SGs from partially fed ticks and observe the effects on infection temporally with greater detail.

Finally, we observed that transfection with dsRNA directed against the transcript for *VNN* reduced virus production in SG cultures infected with POWV-L2 (Fig. 8A and B; see also Fig. S4). This indicated a role for this gene in POWV-L2 infection in an organ critical for virus transmission. It would also be beneficial to identify the *VNN* transcript knockdown effect on TBFV multiplication from SG cultures pretreated with dsRNA and the effect on the multiplication of other TBFVs, such as POWV-L1 and/or LGTV, that are not naturally transmitted by *I. scapularis*. Orthologous mammalian *VNN* has been associated with glycosylphosphatidylinositol (GPI)-linked processes on the cell surfaces (50), vitamin/CoA biosynthetic processes (50), hepatic gluconeogenesis (51, 52), and lipid accumulation (53). Although the structure of human VNN1 has been elucidated (54), very little is known about arthropod orthologs of VNN. There is low (33.9%) amino acid conservation between human VNN1 and the *I. scapularis* ortholog (44); hence, study of whether tick VNN affects cellular TBFV life cycle steps (44), especially within tick SGs, would be worthwhile. Parallel RNA interference (RNAi)–whole-tick studies using multiple TBFVs might be informative, but the durability of transcript knockdown and of the function of the knocked-down transcript may complicate the experiments (55). Thus, careful control of dsRNA application (56) and optimization of other parameters will be crucial. Nonetheless, it will be important to identify whether the *VNN* transcript/protein can functionally reduce not only TBFV infection but also TBFV transmission, an important factor that a candidate target for a vaccine-based or small-molecule-based countermeasure should have (9, 57).

In summary, we showed that *ex vivo* cultures can be used to analyze TBFV infection of SGs from *I. scapularis* in different physiological states. The differences seen in TBV infections of SGs in *in vivo* ticks (25, 38–40) were similarly observed in the cultures. We provided evidence of the presence of virions in vacuoles of individual cells in granular acini of SG cultures from unfed ticks, providing initial insight into possible cellular functions used by infected cells in *I. scapularis* SGs. Additionally, we provided a preliminary observation of TBFV infection in SGs from fed, female *I. scapularis* ticks. Moreover, we provided initial evidence of the involvement of a tick transcript corresponding to *VNN* in POWV-L2 infection by using RNAi-mediated transcript knockdown in SG cultures from both fed and unfed *I. scapularis* female ticks. The SG cultures used represent a convenient system for studying the biology of both the virus and the SG itself.

MATERIALS AND METHODS

***I. scapularis* tick SG dissection and preparation.** Fully engorged, replete (fed) female *I. scapularis* ticks and unfed female *I. scapularis* ticks were obtained from a laboratory colony maintained at the Oklahoma State University (OSU) Tick Rearing Facility. Ticks in different physiological states were housed in humidified desiccators as described by Mitzel et al. (58). Fed ticks were subjected to dissection up to 6 days after receipt from the OSU Tick Rearing Facility (up to 7 days postcollection of blood feeding). Ticks

were aseptically treated by soaking in 3% H_2O_2 for 15 s followed by soaking in 70% ethanol for 15 s (41). After aseptic treatment, ticks were rinsed in three separate pools of sterile phosphate-buffered saline (PBS) on a sterile glass microscope slide and subsequently dissected in sterile PBS on a separate glass microscope slide. L15C-300 medium (59, 60) with no supplemented antibiotics was used for SG culture (41).

SG viability. To determine the viability, or the suggested duration of organ use in culture, data on the metabolic activity of SGs from fed and unfed ticks were collected as described by Grabowski et al. (41). One to three machine replicates (replicate reads from the plate reader) were completed with one SG pair per well and with the corresponding control well that served as a biological replicate. Two to four separate experiments were performed for each organ type ($n = 2$ to 4).

Cell and virus culture. As described before (41), *I. scapularis* ISE6 cells (kindly provided by Timothy Kurtti, University of Minnesota) were cultured at 34°C in complete L15C-300 medium without supplemented antibiotics and CO_2 (80, 81). Vero cells were cultured at 37°C in Dulbecco's modified Eagle's medium (Gibco, Life Technologies, Inc., Carlsbad, CA) supplemented with 10% fetal bovine serum (FBS; Gibco, Life Technologies, Inc., Carlsbad, CA) and with 5% CO_2.

LGTV^{GFP} plasmid construction and rescue of GFP-expressing LGTV (passage 1; used as working stock for experimental infections) was performed as described before (41). Additionally, LGTV^{GFP}, LGTV (TP21 strain), POWV (LB prototype strain; POWV-L1; originally obtained from Robert Tesh, University of Texas Medical Branch), and POWV-DTV (Spooner strain; POWV-L2; a gift from Gregory D. Ebel, Colorado State University) stocks were created as described by Grabowski et al. (41). POWV-L2 stock was also amplified in Vero cells at the same multiplicity of infection (MOI) and grown in the same way as POWV-L1 to provide a working stock for experimental infections. LGTV^{GFP}, LGTV, POWV-L1, and POWV-L2 stock titers were determined in immunofocus assays as described by Offerdahl et al. (48). The same method was used to determine infectious LGTV, POWV-L1, and POWV-L2 titers in experimental samples, with 2 technical replicates per sample. In parallel, a mock stock was prepared from mock-infected Vero cells.

Virus infection of SGs for LGTV^{GFP} expression and infectious virus multiplication. To infect SG cultures with LGTV for subsequent semithin section and transmission electron microscopy (TEM), SGs were dissected as described above and placed into complete L15C-300 medium in wells of a 96-well plate. Using a previously described method (41), a total volume of 5×10^5 focus-forming units (FFU) of LGTV was placed into the infection wells, and mock stock was placed into mock infection wells. Viral adsorption and incubation were completed using a previously described method (41). Organs were collected at 3 and 180 hpi, with processing and staining of organs completed as described below.

To determine levels of infectious POWV-L1 and POWV-L2 multiplication from SG cultures, the culture and infection setup was completed using a previously described method (41). Supernatants were collected from wells with SGs and wells with no SGs at 180 hpi, and virus titers were determined in immunofocus assays as described above, with 2 to 3 separate experiments ($n = 2$ or 3). LGTV^{GFP} infections of a SG pair from a fed tick and an unfed tick under culture conditions were completed with imaging of LGTV^{GFP}-infected SGs as described by Grabowski et al. (41), except that fixation and confocal imaging of infected SGs were completed at 180 hpi (as described below).

Semithin section and transmission electron microscopy imaging of LGTV-infected SGs. LGTV infection and SG collection parameters of mock- and LGTV-infected SGs from fed and unfed ticks were performed as described above. Mock- and LGTV-infected SGs harvested at 3 and 180 hpi (postculture) were fixed in 2.5% glutaraldehyde–4% paraformaldehyde–0.1 M sodium cacodylate buffer (pH 7.4) at 4°C (similarly to a previously reported method [46]) for a minimum of 24 h. Samples were postfixed for 1 h with 0.5% osmium tetroxide–0.8% potassium ferricyanide and stained overnight with 1% uranyl acetate at 4°C, dehydrated with a graded ethanol series. They were further dehydrated with 2×10 min with 100% propylene oxide and then infiltrated and embedded in Epon/araldite resin.

For semithin section imaging, these blocks were sectioned at 1-μm intervals using a Leica RM2265 microtome and diamond knife. Tissue sections were transferred to positively charged slides with a loop and dried at 60°C. Slides were stained with Stevenel's Blue for 10 min at 60°C and air-dried. Coverslips were placed onto the slides and viewed on a Zeiss model AxioVert.A1 microscope at ×40 magnification, and images were captured using a Zeiss model AxioCam 503 mono camera. Images were processed with Zeiss ZEN 2 (blue edition) software using autoexposure settings.

For transmission electron microscopy imaging, the same blocks were sectioned with a Leica UC6 ultramicrotome (Vienna, Austria), stained with 1% uranyl acetate and Reynold's lead citrate, and viewed at 80 kV on a Hitachi 7500 transmission electron microscope (Tokyo, Japan). Digital images were acquired with an AMT digital camera system (AMT, Chazy, NY). Images were processed with Zeiss ZEN 2 (blue edition) software using autoexposure settings.

Confocal imaging of LGTV^{GFP}-infected SGs. Dissection followed by mock and LGTV^{GFP} infection of SGs, performed as described above, was completed. SGs were then collected at 180 hpi and fixed for a minimum of 24 h in 4% paraformaldehyde at 4°C. Individual SGs were washed briefly in 1× PBS following fixation and mounted on microscope slides using ProLong Gold Antifade reagent (Life Technologies) and 12-mm-diameter coverslips (VWR). Mounts were set for at least 24 h at 4°C prior to being imaged on a LSM710 confocal microscope (Zeiss). Images were acquired using a frame size of 2,048 by 2,048 pixels and 1.0× digital zoom with an EC Plan-Neofluar 10×/0.30 numerical aperture (N.A.) or a Plan-Apochromat ×63/1.40 N.A. oil objective. Z stacks used a stack thickness of 1 μm.

Images were observed using Zeiss ZEN v2.3 (blue edition) software. For both mock- and LGTV-infected SGs, ×10 and ×63 images were observed using a software display setting for both red and green channels at settings of 25 and Auto Best Fit, respectively. Z stack images (×10 and ×63) were observed with the software display setting of Auto Best Fit. Movies of the processed Z stack images were recorded with Imaris v8.4.1 software using a gamma correction of 2.0 with both red and green channels at 400 frames.

Preparation of RNA from *I. scapularis* ISE6 cells/SGs and cDNA synthesis. RNA was isolated from ISE6 cells grown using a T25 flask and an RNeasy minikit (Qiagen, Hilden, Germany) and processed according to kit instructions (44). RNA was also isolated as described above from LGTV-infected ISE6 cells by the use of a previously described method (41). For RNA collection from SGs, four and three SG pairs from fed and unfed ticks, respectively, were dissected as described above. The four or three SG pairs were pooled separately in RNAlater (Qiagen) and placed at 4°C for 24 h and then placed at −80°C for longer storage. To extract RNA from SGs from the fed and unfed ticks, RNAlater was carefully removed and replaced with RLT lysis buffer (from the Qiagen RNeasy minikit). SGs were homogenized with Lysing Matrix D tubes (MP Bio) using FastPrep 24 (MP Bio) (42) in the following manner: use of a speed setting of 6 m/s for 40 s, placement on ice for 5 min, and use of a speed setting of 6 m/s for 40 s. The RLT lysis buffer (homogenate) was cleared by centrifugation at 21,000 × *g* for 3 min and placed into columns for further processing as described above according to the manufacturer's instructions for the RNeasy minikit (Qiagen).

cDNA was synthesized from RNA samples using a previously described method (41, 44). An iScript cDNA synthesis kit (Bio-Rad, Hercules, CA, USA) was used, and the following thermocycler conditions were used: 25°C for 5 min, 42°C for 50 min, and 85°C for 5 min.

Synthesis of dsRNA corresponding to pGEM, LGTV 3′UTR, and *I. scapularis VNN*. A T7-tagged cDNA template was generated using a previously described method (41, 44) by using cDNA prepared from a pGEM-T Easy vector DNA plasmid (Promega, Madison, WI), LGTV-infected ISE6 cell RNA, and ISE6 cell RNA with the following T7-tagged primers corresponding to pGEM, the LGTV 3′ untranslated region (3′UTR), and *I. scapularis VNN* (XP_002402506): pGEM forward primer 5′-TAATACGACTCACTATAGGGGG TATCAGCTCACTCAAAGG-3′ and pGEM reverse primer 5′-TAATACGACTCACTATAGGGGAACGACCTACAC CGAACT-3′; LGTV 3′UTR forward primer 5′-TAATACGACTCACTATAGGGCCAGACACAAGGAGTCCAA-3′ and LGTV 3′UTR reverse primer 5′-TAATACGACTCACTATAGGGATGGTGGCTCAGGGAGAAC-3′; *VNN* forward primer 5′-TAATACGACTCACTATAGGGTACCACGGTGACGAGATTGC-3′ and *VNN* reverse primer 5′-T AATACGACTCACTATAGGGTATGTGAGCTCCGCTTGAGG-3′. Two-step PCR was performed under the following thermocycler conditions: 94°C for 5 min; 5 cycles of 94°C for 30 s, 58°C for 30 s, and 72°C for 2 min; 27 cycles of 94°C for 30 s, 68°C for 30 s, and 72°C for 2 min; and final extension at 72°C for 7 min. dsRNA was synthesized from T7-tagged cDNA template using a MEGAscript RNAi synthesis kit according to the manufacturer's instructions and previously described methods (41, 44, 61).

Confirmation of *I. scapularis VNN* transcript in SGs from fed and unfed ticks was completed with cDNA from SGs, *β-actin*/*VNN* primers (*β-actin* forward primer 5′-GAGAAGATGACCCAGATCAT-3′ and *β-actin* reverse primer 5′-TGGTGATCACCTGTCCGTCG-3′ and *VNN* forward primer 5′-TACCACGGTGACGAGATTG C-3′ and *VNN* reverse primer 5′-TATGTGAGCTCCGCTTGAGG-3′), and a PCR (using Phusion high-fidelity PCR master mix with HF buffer [NE Biolabs, Ipswich, USA]) under the following thermocycler conditions: 94°C for 5 min; 32 cycles of 94°C for 30 s, 58°C for 30 s, and 72°C for 2 min; and 72°C for 7 min (44). Following gel electrophoresis on 1.2% Tris-borate-EDTA (TBE) agarose with SYBR Safe (Life Technologies, Carlsbad, CA, USA), the presence of a *VNN* amplicon of the expected size (607 bp) was confirmed (see Fig. S3 in the supplemental material). This *VNN* amplicon was also sequenced from ISE6 cells and an unfed, female *I. scapularis* tick in previous work (44) and confirmed to be highly (96% to 97%) conserved with respect to the *I. scapularis VNN* gene model transcript.

Transfection of infected SGs with dsRNA and transcript knockdown. POWV-L2 infection of SG cultures before overlay of transfection mix was completed as described above for determining infectious TBFV multiplication. Overlay of media and transfection mix was completed as described previously (41, 44, 61). At 108 hpi, supernatants were collected from the POWV-L2-infected, dsRNA-transfected organs and subjected to immunofocus assays (as described above) to determine infectious virus multiplication levels. The time point of 108 h of transfection was utilized due to its being amply efficient for transcript knockdown in tick SG cultures (55, 62), and SGs from both fed and unfed ticks were found to be viable and producing infectious virus.

To determine transcript knockdown following *VNN* dsRNA transfection, three pairs and six pairs of SGs from fed and unfed ticks, respectively, were transfected separately with either *VNN* dsRNA or pGEM dsRNA. All three or six pairs (transfected with either *VNN* or pGEM dsRNA) were pooled to extract RNA and synthesize cDNA as described above. Relative levels of *VNN* transcript was determined using a QuantiFast SYBR green PCR kit (Qiagen) and reverse transcription-quantitative PCR (RT-qPCR) primers relative to the *I. scapularis β-actin* gene (the RT-qPCR primers used were *VNN* forward primer 5′-CTAC AACACCAACGTGGCCT-3′ and *VNN* reverse primer 5′-AAGGGCTCCACAAACAGGTG-3′ and *β-actin* forward primer 5′-GCCGGGACCTTACAGACTATC-3′ and *β-actin* reverse primer 5′-CACGGACAATTTCACGCTCG-3′) (44). Reactions were performed on the Applied Biosystems QuantStudio 6 Flex real-time system (Life Technologies) in Micro-Amp Optical 384-well reaction plates with labeled barcode (Life Technologies). QuantStudio real-time PCR software (v1.3) was used to collect raw threshold cycle (C_T) values, the comparative C_T method ($\Delta\Delta C_T$ method) (44, 63, 64) was used to determine relative transcript expression levels, and an unpaired, two-tailed *t* test was performed with GraphPad Prism (v7.04) software.

SUPPLEMENTAL MATERIAL

Supplemental material for this article may be found at https://doi.org/10.1128/mBio.02628-18.

FIG S1, TIF file, 1.1 MB.
FIG S2, TIF file, 11.1 MB.
FIG S3, TIF file, 1.2 MB.
FIG S4, TIF file, 0.4 MB.
MOVIE S1, MPG file, 2.6 MB.
MOVIE S2, MPG file, 2.4 MB.
MOVIE S3, MPG file, 2.5 MB.
MOVIE S4, MPG file, 2 MB.
MOVIE S5, MPG file, 3.3 MB.
MOVIE S6, MPG file, 4 MB.

ACKNOWLEDGMENTS

We greatly appreciate Lisa Coburn, Cora Vandaveer, Justin Talley, and Phil Mulder (Tick Rearing Facility/National Tick Research and Education Resource/Department of Entomology & Plant Pathology/Oklahoma State University) for aid in shipment and for biological information on the *I. scapularis* colony-based ticks. We thank Ryan Kissinger, Austin Athman, and Anita Mora of the Visual Medical Arts of the Research and Technologies Branch of NIAID/NIH (Hamilton, MT) for aid in graphic art.

This research was supported by the Intramural Research Program of the National Institute of Allergy and Infectious Diseases of the National Institutes of Health.

REFERENCES

1. Rosenberg R, Lindsey NP, Fischer M, Gregory CJ, Hinckley AF, Mead PS, Paz-Bailey G, Waterman SH, Drexler NA, Kersh GJ, Hooks H, Partridge SK, Visser SN, Beard CB, Petersen LR. 2018. Vital signs: trends in reported vectorborne disease cases - United States and territories, 2004–2016. MMWR Morb Mortal Wkly Rep 67:496–501. https://doi.org/10.15585/mmwr.mm6717e1.
2. Hinten SR, Beckett GA, Gensheimer KF, Pritchard E, Courtney TM, Sears SD, Woytowicz JM, Preston DG, Smith RP, Jr, Rand PW, Lacombe EH, Holman MS, Lubelczyk CB, Kelso PT, Beelen AP, Stobierski MG, Sotir MJ, Wong S, Ebel G, Kosoy O, Piesman J, Campbell GL, Marfin AA. 2008. Increased recognition of Powassan encephalitis in the United States, 1999–2005. Vector Borne Zoonotic Dis 8:733–740. https://doi.org/10.1089/vbz.2008.0022.
3. National Academies of Sciences, Engineering, and Medicine. 2016. Global health impacts of vector-borne diseases: workshop summary. The National Academies Press, Washington, DC. https://doi.org/10.17226/21792.
4. Krow-Lucal ER, Lindsey NP, Fischer M, Hills SL. 2018. Powassan virus disease in the United States, 2006–2016. Vector Borne Zoonotic Dis 18:286–290. https://doi.org/10.1089/vbz.2017.2239.
5. Hermance ME, Thangamani S. 2017. Powassan virus: an emerging arbovirus of public health concern in North America. Vector Borne Zoonotic Dis 17:453–462. https://doi.org/10.1089/vbz.2017.2110.
6. Paules CI, Marston HD, Bloom ME, Fauci AS. 2018. Tickborne diseases—confronting a growing threat. N Engl J Med 379:701–703. https://doi.org/10.1056/NEJMp1807870.
7. Dobler G. 2010. Zoonotic tick-borne flaviviruses. Vet Microbiol 140:221–228. https://doi.org/10.1016/j.vetmic.2009.08.024.
8. Ebel GD. 2010. Update on Powassan virus: emergence of a North American tick-borne flavivirus. Annu Rev Entomol 55:95–110. https://doi.org/10.1146/annurev-ento-112408-085446.
9. Grabowski JM, Hill CA. 2017. A roadmap for tick-borne flavivirus research in the "omics" era. Front Cell Infect Microbiol 7:519. https://doi.org/10.3389/fcimb.2017.00519.
10. Fatmi SS, Zehra R, Carpenter DO. 2017. Powassan virus-a new reemerging tick-borne disease. Front Public Health 5:342. https://doi.org/10.3389/fpubh.2017.00342.
11. L'Vov DK, Al'khovskii SV, Shchelkanov M, Deriabin PG, Gitel'man AK, Botikov AG, Aristova VA. 2014. Genetic characterisation of Powassan virus (POWV) isolated from *Haemophysalis longicornis* ticks in Primorye and two strains of Tick-borne encephalitis virus (TBEV) (Flaviviridae, Flavivirus): Alma-Arasan virus (AAV) isolated from *Ixodes persulcatus* ticks in Kazakhstan and Malyshevo virus isolated from *Aedes vexans nipponii* mosquitoes in Khabarovsk kray. Vopr Virusol 59:18–22. (In Russian).
12. Thomas LA, Kennedy RC, Eklund CM. 1960. Isolation of a virus closely related to Powassan virus from *Dermacentor andersoni* collected along North Cache la Poudre River, Colo. Proc Soc Exp Biol Med 104:355–359. https://doi.org/10.3181/00379727-104-25836.
13. McLean DM, Best JM, Mahalingam S, Chernesky MA, Wilson WE. 1964. Powassan virus: summer infection cycle, 1964. Can Med Assoc J 91:1360–1362.
14. McLean DM, Larke RP. 1963. Powassan and Silverwater viruses: ecology of two Ontario arboviruses. Can Med Assoc J 88:182–185.
15. Ebel GD, Kramer LD. 2004. Short report: duration of tick attachment required for transmission of Powassan virus by deer ticks. Am J Trop Med Hyg 71:268–271. https://doi.org/10.4269/ajtmh.2004.71.3.0700268.
16. Costero A, Grayson MA. 1996. Experimental transmission of Powassan virus (Flaviviridae) by *Ixodes scapularis* ticks (Acari:Ixodidae). Am J Trop Med Hyg 55:536–546. https://doi.org/10.4269/ajtmh.1996.55.536.
17. Aliota MT, Dupuis AP, II, Wilczek MP, Peters RJ, Ostfeld RS, Kramer LD. 2014. The prevalence of zoonotic tick-borne pathogens in *Ixodes scapularis* collected in the Hudson Valley, New York state. Vector Borne Zoonotic Dis 14:245–250. https://doi.org/10.1089/vbz.2013.1475.
18. Brackney DE, Nofchissey RA, Fitzpatrick KA, Brown IK, Ebel GD. 2008. Stable prevalence of Powassan virus in *Ixodes scapularis* in a northern Wisconsin focus. Am J Trop Med Hyg 79:971–973. https://doi.org/10.4269/ajtmh.2008.79.971.
19. Campagnolo ER, Tewari D, Farone TS, Livengood JL, Mason KL. 2018. Evidence of Powassan/deer tick virus in adult black-legged ticks (*Ixodes scapularis*) recovered from hunter-harvested white-tailed deer (*Odocoileus virginianus*) in Pennsylvania: a public health perspective. Zoonoses Public Health 65:589–594. https://doi.org/10.1111/zph.12476.
20. Dupuis AP, II, Peters RJ, Prusinski MA, Falco RC, Ostfeld RS, Kramer LD. 2013. Isolation of deer tick virus (Powassan virus, lineage II) from *Ixodes scapularis* and detection of antibody in vertebrate hosts sampled in the Hudson Valley, New York state. Parasit Vectors 6:185. https://doi.org/10.1186/1756-3305-6-185.
21. Knox KK, Thomm AM, Harrington YA, Ketter E, Patitucci JM, Carrigan DR. 2017. Powassan/deer tick virus and *Borrelia Burgdorferi* infection in

Wisconsin tick populations. Vector Borne Zoonotic Dis 17:463–466. https://doi.org/10.1089/vbz.2016.2082.
22. Kuno G, Artsob H, Karabatsos N, Tsuchiya KR, Chang GJ. 2001. Genomic sequencing of deer tick virus and phylogeny of Powassan-related viruses of North America. Am J Trop Med Hyg 65:671–676. https://doi.org/10.4269/ajtmh.2001.65.671.
23. Eisen L. 2018. Pathogen transmission in relation to duration of attachment by *Ixodes scapularis* ticks. Ticks Tick Borne Dis 9:535–542. https://doi.org/10.1016/j.ttbdis.2018.01.002.
24. Alekseev AN, Burenkova LA, Vasilieva IS, Dubinina HV, Chunikhin SP. 1996. Preliminary studies on virus and spirochete accumulation in the cement plug of ixodid ticks. Exp Appl Acarol 20:713–723. https://doi.org/10.1007/BF00051556.
25. Slovak M, Kazimirova M, Siebenstichova M, Ustanikova K, Klempa B, Gritsun T, Gould EA, Nuttall PA. 2014. Survival dynamics of tick-borne encephalitis virus in *Ixodes ricinus* ticks. Ticks Tick Borne Dis 5:962–969. https://doi.org/10.1016/j.ttbdis.2014.07.019.
26. Fielden LJD, Frances D. 2014. Respiratory system, p 240–257. *In* Sonenshine DE, Roe RM (ed), Biology of ticks, vol 2. Oxford University Press, New York, NY.
27. Kim D, Maldonado-Ruiz P, Zurek L, Park Y. 2017. Water absorption through salivary gland type I acini in the blacklegged tick, *Ixodes scapularis*. PeerJ 5:e3984. https://doi.org/10.7717/peerj.3984.
28. Kim D, Simo L, Park Y. 2014. Orchestration of salivary secretion mediated by two different dopamine receptors in the blacklegged tick *Ixodes scapularis*. J Exp Biol 217:3656–3663. https://doi.org/10.1242/jeb.109462.
29. Balashov YS. 1983. Salivary glands, p 98–128. *In* Balashov YS, Raikhel AS, Hoogstraal H (ed), An atlas of ixodid tick ultrastructure. Entomological Society of America, Annapolis, MD.
30. Alarcon-Chaidez FJ. 2014. Salivary glands: structure, physiology, and molecular biology, p 163–205. *In* Sonenshine DE, Roe RM (ed), Biology of ticks, 2nd ed, vol 1. Oxford University Press, Bethesda, MD.
31. Fawcett DW, Binnington K, Voigt WP. 1986. The cell biology of the ixodid tick salivary gland, p 22–45. *In* Sauer JR, Hair JA (ed), Morphology, physiology, and behavioral biology of ticks, vol 1 and 2. Ellis Horwood Limited, Hemstead, Herts, United Kingdom.
32. Walker AR, Fletcher JD, Gill HS. 1985. Structural and histochemical changes in the salivary glands of *Rhipicephalus appendiculatus* during feeding. Int J Parasitol 15:81–100. https://doi.org/10.1016/0020-7519(85)90106-7.
33. Jaworski DC, Muller MT, Simmen FA, Needham GR. 1990. *Amblyomma americanum*: identification of tick salivary gland antigens from unfed and early feeding females with comparisons to *Ixodes dammini* and *Dermacentor variabilis*. Exp Parasitol 70:217–226. https://doi.org/10.1016/0014-4894(90)90102-I.
34. Friesen KJ, Kaufman WR. 2009. Salivary gland degeneration and vitellogenesis in the ixodid tick *Amblyomma hebraeum*: surpassing a critical weight is the prerequisite and detachment from the host is the trigger. J Insect Physiol 55:936–942. https://doi.org/10.1016/j.jinsphys.2009.06.007.
35. Ullah SA, Kaufman WR. 2014. Salivary gland degeneration and ovarian development in the Rocky Mountain wood tick, *Dermacentor andersoni* Stiles (Acari: Ixodidae). I. Post-engorgement events. Ticks Tick Borne Dis 5:569–574. https://doi.org/10.1016/j.ttbdis.2014.03.012.
36. Ullah SA, Kaufman WR. 2014. Salivary gland degeneration and ovary development in the Rocky Mountain wood tick, *Dermacentor andersoni* Stiles (Acari: Ixodidae). II. Determination of the 'critical weight'. Ticks Tick Borne Dis 5:516–522. https://doi.org/10.1016/j.ttbdis.2014.03.007.
37. Yu X, Zhou Y, Cao J, Zhang H, Gong H, Zhou J. 2017. Caspase-1 participates in apoptosis of salivary glands in *Rhipicephalus haemaphysaloides*. Parasit Vectors 10:225. https://doi.org/10.1186/s13071-017-2161-1.
38. Dickson DL, Turell MJ. 1992. Replication and tissue tropisms of Crimean-Congo hemorrhagic fever virus in experimentally infected adult *Hyalomma truncatum* (Acari: Ixodidae). J Med Entomol 29:767–773. https://doi.org/10.1093/jmedent/29.5.767.
39. Belova OA, Burenkova LA, Karganova GG. 2012. Different tick-borne encephalitis virus (TBEV) prevalences in unfed versus partially engorged ixodid ticks–evidence of virus replication and changes in tick behavior. Ticks Tick Borne Dis 3:240–246. https://doi.org/10.1016/j.ttbdis.2012.05.005.
40. Booth TF, Davies CR, Jones LD, Staunton D, Nuttall PA. 1989. Anatomical basis of Thogoto virus infection in BHK cell culture and in the ixodid tick vector, *Rhipicephalus appendiculatus*. J Gen Virol 70:1093–1104. https://doi.org/10.1099/0022-1317-70-5-1093.
41. Grabowski JM, Tsetsarkin KA, Long D, Scott DP, Rosenke R, Schwan TG, Mlera L, Offerdahl DK, Pletnev AG, Bloom ME. 2017. Flavivirus infection of *Ixodes scapularis* (black-legged tick) *ex vivo* organotypic cultures and applications for disease control. mBio 8:e01255-17. https://doi.org/10.1128/mBio.01255-17.
42. McNally KL, Mitzel DN, Anderson JM, Ribeiro JM, Valenzuela JG, Myers TG, Godinez A, Wolfinbarger JB, Best SM, Bloom ME. 2012. Differential salivary gland transcript expression profile in *Ixodes scapularis* nymphs upon feeding or flavivirus infection. Ticks Tick Borne Dis 3:18–26. https://doi.org/10.1016/j.ttbdis.2011.09.003.
43. Liu XY, Bonnet SI. 2014. Hard tick factors implicated in pathogen transmission. PLoS Negl Trop Dis 8:e2566. https://doi.org/10.1371/journal.pntd.0002566.
44. Grabowski JM, Gulia-Nuss M, Kuhn RJ, Hill CA. 2017. RNAi reveals proteins for metabolism and protein processing associated with Langat virus infection in *Ixodes scapularis* (black-legged tick) ISE6 cells. Parasit Vectors 10:24. https://doi.org/10.1186/s13071-016-1944-0.
45. Grabowski JM, Offerdahl DK, Bloom ME. 2018. The use of *ex vivo* organ cultures in tick-borne virus research. ACS Infect Dis 4:247–256. https://doi.org/10.1021/acsinfecdis.7b00274.
46. Gill HS, Walker AR. 1987. The salivary glands of *Hyalomma anatolicum anatolicum*: structural changes during attachment and feeding. Int J Parasitol 17:1381–1392. https://doi.org/10.1016/0020-7519(87)90074-9.
47. Kim D, Urban J, Boyle DL, Park Y. 2016. Multiple functions of Na/K-ATPase in dopamine-induced salivation of the blacklegged tick, *Ixodes scapularis*. Sci Rep 6:21047. https://doi.org/10.1038/srep21047.
48. Offerdahl DK, Dorward DW, Hansen BT, Bloom ME. 2012. A three-dimensional comparison of tick-borne flavivirus infection in mammalian and tick cell lines. PLoS One 7:e47912. https://doi.org/10.1371/journal.pone.0047912.
49. Engelhard EK, Kam-Morgan LN, Washburn JO, Volkman LE. 1994. The insect tracheal system: a conduit for the systemic spread of *Autographa californica* M nuclear polyhedrosis virus. Proc Natl Acad Sci U S A 91:3224–3227. https://doi.org/10.1073/pnas.91.8.3224.
50. Kaskow BJ, Proffitt JM, Michael Proffit J, Blangero J, Moses EK, Abraham LJ. 2012. Diverse biological activities of the vascular non-inflammatory molecules - the Vanin pantetheinases. Biochem Biophys Res Commun 417:653–658. https://doi.org/10.1016/j.bbrc.2011.11.099.
51. Chen S, Zhang W, Tang C, Tang X, Liu L, Liu C. 2014. Vanin-1 is a key activator for hepatic gluconeogenesis. Diabetes 63:2073–2085. https://doi.org/10.2337/db13-0788.
52. van Diepen JA, Jansen PA, Ballak DB, Hijmans A, Rutjes FP, Tack CJ, Netea MG, Schalkwijk J, Stienstra R. 2016. Genetic and pharmacological inhibition of vanin-1 activity in animal models of type 2 diabetes. Sci Rep 6:21906. https://doi.org/10.1038/srep21906.
53. Motomura W, Yoshizaki T, Takahashi N, Kumei S, Mizukami Y, Jang SJ, Kohgo Y. 2012. Analysis of vanin-1 upregulation and lipid accumulation in hepatocytes in response to a high-fat diet and free fatty acids. J Clin Biochem Nutr 51:163–169. https://doi.org/10.3164/jcbn.12-06.
54. Boersma YL, Newman J, Adams TE, Cowieson N, Krippner G, Bozaoglu K, Peat TS. 2014. The structure of vanin 1: a key enzyme linking metabolic disease and inflammation. Acta Crystallogr D Biol Crystallogr 70:3320–3329. https://doi.org/10.1107/S1399004714022767.
55. Karim S, Miller NJ, Valenzuela J, Sauer JR, Mather TN. 2005. RNAi-mediated gene silencing to assess the role of synaptobrevin and cystatin in tick blood feeding. Biochem Biophys Res Commun 334:1336–1342. https://doi.org/10.1016/j.bbrc.2005.07.036.
56. de la Fuente J, Kocan KM, Almazán C, Blouin EF. 2007. RNA interference for the study and genetic manipulation of ticks. Trends Parasitol 23:427–433. https://doi.org/10.1016/j.pt.2007.07.002.
57. Labuda M, Trimnell AR, Lickova M, Kazimirova M, Davies GM, Lissina O, Hails RS, Nuttall PA. 2006. An antivector vaccine protects against a lethal vector-borne pathogen. PLoS Pathog 2:e27. https://doi.org/10.1371/journal.ppat.0020027.
58. Mitzel DN, Wolfinbarger JB, Long RD, Masnick M, Best SM, Bloom ME. 2007. Tick-borne flavivirus infection in *Ixodes scapularis* larvae: development of a novel method for synchronous viral infection of ticks. Virology 365:410–418. https://doi.org/10.1016/j.virol.2007.03.057.
59. Munderloh UG, Liu Y, Wang M, Chen C, Kurtti TJ. 1994. Establishment, maintenance and description of cell lines from the tick *Ixodes scapularis*. J Parasitol 80:533–543. https://doi.org/10.2307/3283188.

60. Munderloh UG, Kurtti TJ. 1989. Formulation of medium for tick cell culture. Exp Appl Acarol 7:219–229. https://doi.org/10.1007/BF01194061.
61. Barry G, Alberdi P, Schnettler E, Weisheit S, Kohl A, Fazakerley JK, Bell-Sakyi L. 2013. Gene silencing in tick cell lines using small interfering or long double-stranded RNA. Exp Appl Acarol 59:319–338. https://doi.org/10.1007/s10493-012-9598-x.
62. Karim S, Ramakrishnan VG, Tucker JS, Essenberg RC, Sauer JR. 2004. *Amblyomma americanum* salivary glands: double-stranded RNA-mediated gene silencing of synaptobrevin homologue and inhibition of PGE2 stimulated protein secretion. Insect Biochem Mol Biol 34:407–413. https://doi.org/10.1016/j.ibmb.2004.01.005.
63. Livak KJ, Schmittgen TD. 2001. Analysis of relative gene expression data using real-time quantitative PCR and the 2(-Delta Delta C(T)) method. Methods 25:402–408. https://doi.org/10.1006/meth.2001.1262.
64. Rao X, Huang X, Zhou Z, Lin X. 2013. An improvement of the 2^(-delta delta CT) method for quantitative real-time polymerase chain reaction data analysis. Biostat Bioinforma Biomath 3:71–85.
65. Grabowski JM, Perera R, Roumani AM, Hedrick VE, Inerowicz HD, Hill CA, Kuhn RJ. 2016. Changes in the proteome of Langat-infected *Ixodes scapularis* ISE6 cells: metabolic pathways associated with flavivirus infection. PLoS Negl Trop Dis 10:e0004180. https://doi.org/10.1371/journal.pntd.0004180.